Neurobiology of Aging 76 (2019) 35–44

Contents lists available at ScienceDirect

Neurobiology of Aging

journal homepage: www.elsevier.com/locate/neuaging

DNA methylation variability in Alzheimer's disease

Zhiguang Huo [a], Yun Zhu [b], Lei Yu [c], Jingyun Yang [c], Philip De Jager [d], David A. Bennett [c], Jinying Zhao [b,*]

[a] Department of Biostatistics, University of Florida, Gainesville, FL, USA
[b] Department of Epidemiology, University of Florida, Gainesville, FL, USA
[c] Rush Alzheimer's Disease Center, Rush University Medical Center, Chicago, IL, USA
[d] Department of Neurology, College of Physicians & Surgeons, Columbia University, NY, USA

ARTICLE INFO

Article history:
Received 19 July 2018
Received in revised form 7 November 2018
Accepted 12 December 2018
Available online 21 December 2018

Keywords:
DNA methylation variability
Alzheimer's disease
Amyloid-β plaques
PHF-tau tangles
Postmortem brain
PFC
ROSMAP

ABSTRACT

DNA methylation plays a critical role in brain aging and Alzheimer's disease (AD). While prior studies have largely focused on testing mean DNA methylation, DNA methylation instability (quantified by DNA methylation variability) may also affect disease susceptibility. Using DNA methylation data collected by the Religious Orders Study and the Rush Memory and Aging Project, we identified 249 and 115 variably methylated probes (VMPs) associated with amyloid-β and neurofibrillary tangles, respectively. These VMPs clustered into 133 and 14 regions, respectively. Notably, we found that most of these VMPs did not overlap with differentially methylated probes, indicating that VMPs and differentially methylated probes may capture different sets of genes associated with AD pathology. Overall, our results demonstrated that DNA methylation instability affects AD neuropathology and highlights the importance of testing methylation variability in epigenetic research.

1. Introduction

Alzheimer's dementia is a devastating neurodegenerative disorder affecting over 35 million people worldwide, and this number is expected to nearly triple by 2050 (Duthey, 2013). Accumulation of extracellular amyloid-β and intraneuronal neurofibrillary tangles are the 2 hallmarks of Alzheimer's disease (AD). DNA methylation plays an important role in regulating gene expression, and altered DNA methylation has been implicated in AD pathology (Irier and Jin, 2012). Several epigenome-wide association studies (De Jager et al., 2014; Lunnon et al., 2014; Smith et al., 2018; Watson et al., 2016) identified differentially methylated probes (DMPs) and differentially methylated regions associated with AD. While previous studies have largely focused on testing the difference in mean DNA methylation level between patients and controls, recent evidence suggests that DNA methylation instability may also affect disease susceptibility (Palumbo et al., 2018). For example, several recent studies found that increased DNA methylation variability in multiple genes was associated with cancers (Hansen et al., 2011), type 1 diabetes (Paul et al., 2016), aging (Jones et al., 2015), and rheumatoid arthritis (Webster et al., 2018). This evidence suggests that, in addition to the mean change in DNA methylation, altered DNA methylation variability or instability of DNA methylation may also play an important role in disease pathophysiology. To date, we are not aware of any study that examined the role of DNA methylation variability in AD neuropathology. Using existing DNA methylation and gene expression data generated in postmortem prefrontal cortex of older individuals participating in 2 community-based population cohorts of aging and dementia (the Religious Orders Study and the Rush Memory and Aging Project [ROSMAP]) (Bennett et al., 2012b), we conducted analyses to examine whether altered DNA methylation stability contributes to AD pathology by identifying variably methylated probes (VMPs) and variably methylated regions (VMRs) in the postmortem brain tissue. For comparison purpose, we also examined the potential overlap between variably methylated genes (e.g., genes showing altered methylation variability) and differentially methylated genes (e.g., genes showing altered mean DNA methylation level) at a genome scale. Moreover, we assessed the impact of DNA methylation instability on gene expression profiled on the same brain cortex.

* Corresponding author at: Department of Epidemiology, College of Public Health and Health Professions, College of Medicine, University of Florida 2004 Mowry Road, Gainesville, FL 32610. Tel.: +1 352 273 5933; fax: +1 352 273 5365.
E-mail address: jzhao66@ufl.edu (J. Zhao).

0197-4580/$ – see front matter © 2018 Elsevier Inc. All rights reserved.
https://doi.org/10.1016/j.neurobiolaging.2018.12.003

2. Materials and methods

2.1. Study population

This study included deceased participants from 2 ongoing, prospective studies of brain aging and dementia in older individuals, as described in the following. Detailed study design and assessment methods were described previously (Bennett et al., 2006, 2012a,b). Both studies were approved by the Institutional Review Board of the Rush University Medical Center. Data are available for sharing at www.radc.rush.edu. Clinical characteristics of the study participants at the time of death are shown in Table 1. The mean (SD) age of brain donors was 88.0 (6.7) years at the time of death. Men account for 37% of the study participants, and AD accounts for 42%.

2.1.1. Religious Orders Study

Initiated in 1994, Religious Orders Study (ROS) enrolled older Catholic priests, nuns, and brothers from across the U.S. free of known dementia at time of enrollment. Participants agreed to annual clinical evaluations including standardized neurological examination and neuropsychological testing and signed both an informed consent and an Anatomic Gift Act donating their brains at the time of death (Bennett et al., 2006, 2012a). Both the follow-up rate of survivors and the autopsy rate exceed 90% (autopsies of deaths).

2.1.2. Rush Memory and Aging Project

Established in 1997, Memory and Aging Project (MAP) consists of older men and women from across the Chicagoland area, without known dementia at enrollment. Participants agreed to annual clinical evaluations and signed both an informed consent and an Anatomic Gift Act donating their brains, spinal cords, and selected nerves and muscles at the time of death (Bennett et al., 2006, 2012b). The follow-up rate for survivors exceeds 90%, and the autopsy rate for deceased subjects exceeds 80% (autopsies of deaths).

2.2. Assessment of neuropathological phenotypes

We collected comprehensive neuropathological phenotypes for brain aging and AD in ROSMAP by a same team of investigators using a large common core of testing batteries. Thus, data can be efficiently merged for joint analyses. Detailed methods for clinical phenotyping have been described previously (Bennett et al., 2006, 2009). The quantitative AD pathologic burden (our primary outcomes) includes the overall amyloid-β load based on percent area occupied with image analysis, and the density of paired helical filament tau tangles assessed with stereology, which were identified by molecularly specific immunohistochemistry and quantified by imaging analysis. These 2 composite summary measures were obtained by averaging the percent area occupied by amyloid-β or tangles across 8 regions, as previously described (Bennett et al., 2004). Neuropathologic examinations were made by board-certified neuropathologists blinded to the clinical data.

Table 1
Clinical characteristics of the brain donors (N = 706)

Characteristics	% or mean ±SD
Age (y)	88.0 ± 6.7
Males (%)	261 (37.0)
Education level (y)	16.4 ± 3.6
Study affiliation (MAP, %)	326 (46.2)
MMSE score	15.8±10.2
PMI (hours)	7.5 ± 5.9
AD	298 (42.2)
PHF tau tangles[a]	6.4 ± 8.1
Amyloid-β plaques[b]	1.4 ± 1.1

Key: AD, Alzheimer's disease; MAP, Memory and Aging Project; PHF, paired helical filament.
[a] Mean of PHF tau tangles score in 8 brain regions.
[b] Mean of amyloid-β score (square root transformed) in 8 brain regions.

2.3. Assessment of cognitive performance

During each annual clinical visit, participants received evaluations of their cognition functions via a battery of 21 cognitive performance tests across a range of cognitive abilities. Nineteen of them were used to construct a global composite measure of cognitive function and summarized as 5 cognitive domains including episode memory, working memory, semantic memory, perceptual speed, and visuospatial ability. Detailed methods for the assessment of cognitive functions in ROSMAP cohorts have been described previously (Bennett et al., 2012a; Wilson et al., 2015).

2.4. DNA methylation data preprocessing

DNA methylation in the dorsolateral prefrontal cortex was measured using Infinium HumanMethylation450 BeadChip as previously described (De Jager et al., 2014). Data preprocessing, QC, and normalization were performed using the RnBeads software (Assenov et al., 2014) with default options unless otherwise stated. Of the 732 subjects and 474,841 autosomal CpG probes, we removed probes and/or subjects based on the following criteria: (1) samples with low bisulfite conversion rate (De Jager et al., 2014) (n = 21); (2) outliers determined by PCA analysis (De Jager et al., 2014) (n = 5); (3) 14,018 probes located within ±5 bp of known SNPs (MAF > 0.05); (4) 5473 probes using SNP criterion "3," 10,588 probes with high median detection *p*-values ($p > 0.05$), and 2804 probes with nonacceptable context based on the *RnBeads* default options. Data normalization was performed using the "*swan*" method implemented in the *RnBeads* software. Our final data analysis included a total of 441,958 probes and 706 subjects. Missing values were computed by the *KNN* algorithm with k = 100 using R package *impute* (Hastie et al., 2001) from Bioconductor.

2.5. Identifying VMPs/VMRs associated with AD neuropathology

To identify VMPs associated with AD pathology, we used the *DiffVar* function (Phipson and Oshlack, 2014) implemented in the *missMethyl* package (Phipson et al., 2015). In this analysis, we adjusted for age at death, sex, batch, study (ROS or MAP), and education level. Given the high correlation of DNA methylation between adjacent CpG sites, disease-related CpGs can be clustered in genomic regions, and we thus also performed region-based analysis to identify VMRs associated with amyloid-β, tangles, separately, using a 5kb sliding window approach. Statistical significance of a VMR was obtained by combining *p*-values (from *DiffVar*) of all CpG probes within each 5kb window using the *Brown's* method (Brown, 1975) implemented in the R package *empiricalBrownsMethod* (Poole et al., 2016), which takes into account the correlation between adjacent probes. Multiple testing was controlled by the false discovery rate (FDR) (Benjamini and Hochberg, 1995) and a *q*-value <0.05 was used to determine statistical significance for both VMP and VMR analyses. A more stringent genome-wide estimate of significance level $\alpha = 3.6 \times 10^{-8}$ (Saffari et al., 2018) was adopted in the volcano plot in addition to the *q*-value < 0.05 criteria.

2.6. VMPs/VMRs associated with cognitive performance

To identify VMPs/VMRs associated with cognitive performance, we used the same statistical methods with adjustments for same covariates. The cognitive performance was quantified by the composite measure of cognitive functions proximate to death, including global cognitive function, episode memory, working memory, semantic memory, perceptual speed, or visuospatial ability.

2.7. Sensitivity analyses

To examine whether and how nonlinear effect of age affects methylation variation, we additionally adjusted for age^2 and age^3 (age at death). To examine whether neuronal cell proportions influence our results, we first estimated the NeuN+ cells (primary neurons) proportion using the *projectCellType* function in the *minfi* R package (Aryee et al., 2014) based on the dorsolateral prefrontal cortex cell epigenotype reference database (Guintivano et al., 2013) and then additionally adjusted for neurons proportions in the statistical models. To examine whether population substructure affects our results, we calculated the genomic inflation factors using the R package *QQperm* (Yang et al., 2011).

2.8. Functional annotation and validation

To explore the potential functions of the identified VMPs/VMRs, we first annotated them to genomic features using the *GenomicFeatures* package in Bioconductor (Lawrence et al., 2013). We then tested the association between gene expression (RNA-seq in same brain cortex) of VMPs and AD neuropathology using the *limma* function in R (Smyth, 2005). We focused on *cis*-regulation (±5 kb of a tested VMP) and adjusted for age at death, sex, batch, study (ROS or MAP), and education level. Functional enrichment analysis was conducted using the Kolmogorov Smirnov test (KS-test) (Stephens, 1974), a nonparametric approach that does not require an arbitrary cutoff to claim significance. In this analysis, we considered 2 pathway databases: (1) curated genes based on the Molecular Signatures Database v6.1 (http://software.broadinstitute.org/gsea/msigdb/index.jsp), including Biocarta, KEGG, Reactome, and Gene ontology (GO) and (2) previously published GWAS loci (a.k.a. GWAS catalog (Welter et al., 2013) and genes/proteins known to be involved in AD pathology (Campion et al., 2016). Pathways with less than 10 or greater than 400 genes were excluded from the enrichment analysis. Multiple testing was corrected for total number of pathways using FDR, and $q < 0.05$ was considered as statistically significant.

2.9. Co-methylation networks

To examine whether genes that are differentially variably methylated in relation to AD neuropathology are co-methylated, we conducted the Weighted Gene Correlation Network Analysis (Langfelder and Horvath, 2008). This analysis included a total of 1145 or 967 VMPs showing nominal associations ($p < 0.001$) with amyloid-β or tangles, respectively. Co-methylation modules were constructed separately among subjects with high (upper tertile) versus low (bottom tertile) pathological burden for each measure. Differential networks—modules vary by pathological burden—were identified by comparing the 2 groups via preservation analysis in the Weighted Gene Correlation Network Analysis. Hub genes within each co-methylation modules were detected using the *ARACNE* algorithm (Margolin et al., 2006) in the R package *minet* (Meyer et al., 2008). Network visualization was done using the R package *igraph* (Csardi and Nepusz, 2006).

2.10. Overlapping between VMPs and DMPs

To examine whether and to what extent the identified VMPs overlapped with DMPs in relation to AD pathology, we performed differential methylation analysis to identify DMPs associated with AD neuropathology using R package *limma* (Smyth, 2005), adjusting for same covariates as what used in the VMP analysis.

2.11. Replication

To replicate our findings in the ROSMAP cohort, we downloaded DNA methylation data from the publicly available data set GSE80970 (n = 142, mean age 85.7, 38% men). The data contain DNA methylation data (450K array) in dorsolateral prefrontal cortex (same brain region as that in ROSMAP) and clinical information for Braak (a semiquantitative measure for tangle), age, and gender. Detailed information for this data set has been described previously (Smith et al., 2018). As the data did not include phenotype information for amyloid, we focused on replication of tangle-related VMPs only.

3. Results

3.1. VMPs/VMRs associated with AD neuropathology

At the level of $q < 0.05$, we identified 249 VMPs (223 hypervariable [i.e., greater variability with more neuropathology], 26 hypovariable [i.e., less variability with more neuropathology]) associated with amyloid-β load (Fig. 1A). By contrast, 115 VMPs (48 hypervariable, 67 hypovariable) were associated with tangles (Fig. 1B). Tables 2 and 3 list the top 50 most significant VMPs associated with amyloid-β and tangles, respectively. The identified VMPs are clustered into 133 and 14 VMRs for amyloid-β and tangles, respectively. A full list of the VMPs/VMRs associated with amyloid-β and tangles is shown in the online Tables S1 and S2, respectively.

3.2. VMPs associated with cognitive performance

We identified 1 VMP associated with global cognitive function, 6 VMPs associated with semantic memory, and 14 VMPs with working memory at FDR 5% (Tables S3).

3.3. Sensitivity analyses

After additional adjustment for nonlinear age effect (Table S4) or cell proportions (Tables S5), the identified VMPs remain to be significant, indicating that the observed associations of VMPs with AD pathology are unlikely to be confounded by these factors. In addition, the genomic inflation factors were 1.02 for tangles and 1.06 for amyloid-β, indicating that population stratification did not confound our results either.

3.4. Genomic distribution of the identified VMPs

To explore the potential functional impact of the VMPs on transcriptional activities, we annotated the identified VMPs to predetermined genomic features (Fig. 2). Compared to the null distribution of CpG probes included in the Illumina HumanMethylation450 array, VMPs associated with amyloid-β were significantly enriched in introns (15% vs. 21%, $p < 0.001$) and intergenic regions (57% vs. 66%, $p < 0.001$), but depleted in promoter regions (23% vs. 8.4%, $p < 0.001$). By contrast, VMPs associated with tangles were overrepresented in promoter regions (23% vs. 31%, $p = 0.001$) but depleted in intergenic regions (57% vs. 51%, $p = 0.001$). Fig. S3 shows the distributions of methylation variability

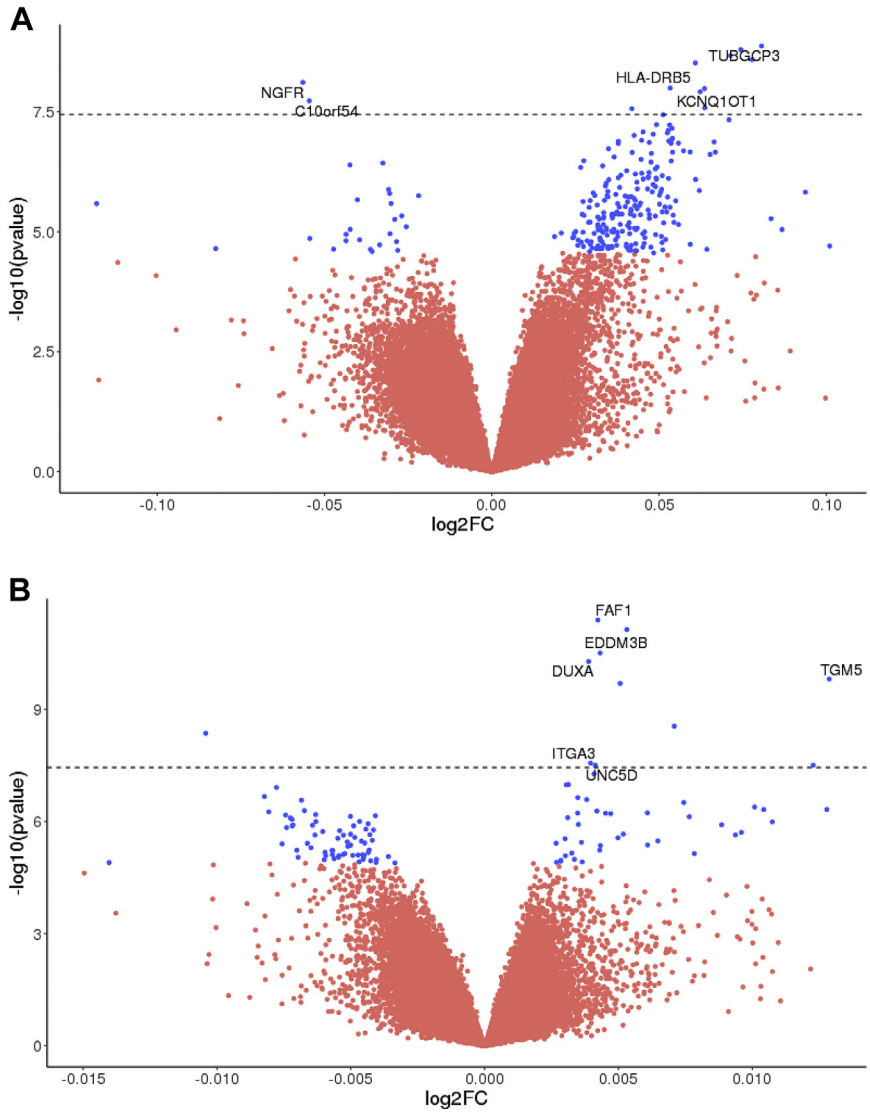

Fig. 1. Volcano plots showing the identified VMPs associated with amyloid plaques (A) and tangles (B). The *p*-values in −log10 scale (Y-axis) are plotted against the log2 fold change (log2FC) of variability with respect to unit increase of the pathological burden (X-axis). A positive log2FC represents hypervariable methylation, and a negative log2FC represents hypovariable methylation. The VMPs with q < 0.05 are marked with the blue color and the VMPs with q > 0.05 are marked with the red color. The dashed horizontal line represents genome-wide significance level $\alpha = 3.6 \times 10^{-8}$, and the VMPs with $p < 3.6 \times 10^{-8}$ are annotated by genes within ±5 kb of the probe. Abbreviation: VMPs, variably methylated probes. (For interpretation of the references to color in this figure legend, the reader is referred to the Web version of this article.)

status (hypervariable vs. hypovariable) for the identified VMPs with respect to genomic locations (promoters, intergenic regions, introns, and exons) and/or neuropathological features (tangle vs. amyloid). It shows that (1) a large proportion of tangle-related VMPs are hypovariably methylated (58% hypo vs. 42% hyper), and these VMPs are more likely to be located in promoters (36% vs. 23%), and less likely to be located in exons (1% vs. 5%), introns (10% vs. 15%), and intergenic regions (52% vs. 57%), as compared to the null distribution of the CpG probes in the Illumina HumanMethylation450 array. (2) Most of the amyloid-related VMPs are hypervariable (90% hyper vs. 10% hypo), and these VMPs are more likely to be located in intergenic regions (70% vs. 57%), followed by introns (21% vs. 15%), exons (1% vs. 5%), and promoters (9% vs. 23%), after adjusting for the null distribution of the CpG probes on the chip. To further examine whether this differential association (i.e., tangle-related VMPs are more likely to be hypovariable, whereas amyloid-related VMPs are more likely to be hypervariable) is confounded by genomic locations, we fitted a logistic regression model, in which methylation variability status (hypervariable or hypovariable, y/n) was the dependent variable, and a neuropathological trait of interest (tangle or amyloid) was the independent variable, adjusting for genomic locations. We found that the observed differential association of DNA methylation variability status with AD neuropathology is independent of genomic locations of the probes (p-value $= 1.32 \times 10^{-16}$). These findings support a role of DNA methylation instability in AD pathology and demonstrated that DNA methylation variability is trait specific. The differential genomic distributions for amyloid-related and tangle-related VMPs also suggest that these 2 hallmarks of AD are etiologically heterogeneous.

3.5. Functional validation by RNA-seq

Using RNA-seq data profiled from the same brain neocortical regions, we examined whether the identified VMPs/VMRs affected gene expression. We found that, of the 115 VMPs (annotated to 70

Table 2
Top 50 most significant variably methylated probes (VMPs) associated with amyloid-β (q < 0.05)

CpG probe	Chr	Position (bps)	Genomic feature	*p*-value	*q*-value	Gene[a]	Direction[b]
cg01624068	13	113,137,799	Intergenic	1.35×10^{-9}	2.68×10^{-4}	*TUBGCP3*	↑
cg10506070	5	114,502,492	Intergenic	1.60×10^{-9}	2.68×10^{-4}		↑
cg00391025	3	100,427,239	Intergenic	2.13×10^{-9}	2.68×10^{-4}		↑
cg19734937	2	63,855,048	Intergenic	2.58×10^{-9}	2.68×10^{-4}		↑
cg25871696	13	81,914,087	Intergenic	3.03×10^{-9}	2.68×10^{-4}		↑
cg26102082	17	47,590,272	Exons	7.70×10^{-9}	5.67×10^{-4}	*NGFR*	↓
cg06060962	6	32,515,150	Introns	1.01×10^{-8}	5.75×10^{-4}	*HLA-DRB5*	↑
cg02226953	7	150,525,449	Intergenic	1.04×10^{-8}	5.75×10^{-4}		↑
cg03660952	11	2,644,418	Exons	1.21×10^{-8}	5.93×10^{-4}	*KCNQ1OT1*	↑
cg23968456	10	73,521,631	Exons	1.87×10^{-8}	8.25×10^{-4}	*C10orf54*	↓
cg14313916	8	8,640,017	Intergenic	2.61×10^{-8}	1.00×10^{-3}		↑
cg15948245	7	104,581,746	Promoters	2.72×10^{-8}	1.00×10^{-3}		↑
cg21110873	12	131,712,414	Intergenic	3.66×10^{-8}	1.24×10^{-3}		↑
cg19550439	5	64,470,134	Introns	4.64×10^{-8}	1.47×10^{-3}	*ADAMTS6*	↑
cg23493751	3	46,204,787	Promoters	5.86×10^{-8}	1.65×10^{-3}	*CCR3*	↑
cg25814432	19	54,620,431	Introns	5.97×10^{-8}	1.65×10^{-3}	*PRPF31*	↑
cg17917920	7	93,220,788	Intergenic	7.00×10^{-8}	1.82×10^{-3}		↑
cg13501912	3	87,424,518	Intergenic	7.72×10^{-8}	1.90×10^{-3}		↑
cg06890950	4	81,382,711	Introns	8.28×10^{-8}	1.93×10^{-3}	*C4orf22*	↑
cg08041573	21	33,651,723	Intergenic	8.72×10^{-8}	1.93×10^{-3}		↑
cg03043928	11	2,085,203	Intergenic	9.28×10^{-8}	1.95×10^{-3}		↑
cg21002735	11	77,350,306	Intergenic	9.85×10^{-8}	1.98×10^{-3}	*CLNS1A*	↑
cg07725198	1	27,229,130	Intergenic	1.13×10^{-7}	2.00×10^{-3}	*GPATCH3*	↑
cg09609314	2	174,147,631	Intergenic	1.20×10^{-7}	2.00×10^{-3}		↑
cg18677996	5	17,031,869	Intergenic	1.25×10^{-7}	2.00×10^{-3}		↑
cg10655371	7	91,749,682	Introns	1.29×10^{-7}	2.00×10^{-3}	*CYP51A1*	↑
cg20996620	7	20,623,878	Intergenic	1.30×10^{-7}	2.00×10^{-3}		↑
cg06931905	8	42,036,940	Intergenic	1.35×10^{-7}	2.00×10^{-3}		↑
cg00689014	17	39,869,138	Introns	1.38×10^{-7}	2.00×10^{-3}	*JUP*	↑
cg13290719	4	58,063,449	Introns	1.43×10^{-7}	2.00×10^{-3}	*IGFBP7-AS1*	↑
cg10575940	17	75,365,389	Intergenic	1.44×10^{-7}	2.00×10^{-3}		↑
cg07561890	2	133,036,548	Intergenic	1.45×10^{-7}	2.00×10^{-3}		↑
cg16608672	5	30,346,809	Intergenic	1.86×10^{-7}	2.49×10^{-3}		↑
cg14446166	7	148,934,349	Intergenic	2.05×10^{-7}	2.60×10^{-3}		↑
cg27340958	4	7,755,730	Promoters	2.19×10^{-7}	2.60×10^{-3}	*AFAP1-AS1*	↑
cg26529712	19	35,399,253	Intergenic	2.20×10^{-7}	2.60×10^{-3}		↑
cg26879538	6	30,014,916	Introns	2.21×10^{-7}	2.60×10^{-3}	*ZNRD1ASP*	↑
cg03318222	19	56,847,740	Introns	2.24×10^{-7}	2.60×10^{-3}	*ZSCAN5A*	↑
cg21512370	13	48,990,327	Introns	2.34×10^{-7}	2.65×10^{-3}	*LPAR6*	↑
cg12447346	1	161,055,663	Introns	2.45×10^{-7}	2.70×10^{-3}	*NECTIN4*	↑
cg27616595	7	146,484,518	Intergenic	2.77×10^{-7}	2.98×10^{-3}		↑
cg01481116	11	93,867,992	Introns	3.11×10^{-7}	3.27×10^{-3}	*PANX1*	↑
cg14519534	7	102,082,149	Introns	3.32×10^{-7}	3.36×10^{-3}	*ORAI2*	↑
cg24620463	7	95,917,902	Intergenic	3.35×10^{-7}	3.36×10^{-3}		↑
cg20185525	17	41,278,712	Introns	3.54×10^{-7}	3.48×10^{-3}	*BRCA1*	↑
cg21775279	1	28,285,385	Exons	3.71×10^{-7}	3.56×10^{-3}	*SMPDL3B*	↓
cg03169557	16	89,598,950	Exons	4.05×10^{-7}	3.80×10^{-3}	*SPG7*	↓
cg02180296	14	24,404,306	Intergenic	4.24×10^{-7}	3.90×10^{-3}	*DHRS4-AS1*	↑
cg02312525	22	50,525,778	Intergenic	4.48×10^{-7}	4.04×10^{-3}	*MLC1*	↑
cg19988798	5	175,511,300	Intergenic	4.58×10^{-7}	4.05×10^{-3}		↑

[a] The nearest annotated gene within ±5kb of the CpG probe.
[b] ↑ indicates hypervariability (increased variability in subjects with higher neuropathological burden as compared to those with lower burden), and ↓ indicates hypovariability (decreased variability in subjects with higher neuropathological burden as compared to those with lower burden).

unique genes) associated with tangles, 35 genes were also differentially expressed ($q < 0.05$), whereas of the 249 VMPs (annotated to 113 unique genes) associated with amyloid-β, only 2 genes showed differential expression ($q < 0.05$). Genes showing both differential variability and differential expression are listed in the Table S6. Although these results demonstrated that the identified VMPs might affect gene expression, the seemingly larger effect of tangle-related VMPs, as compared to amyloid-β-related VMPs, on gene expression deserves further investigation.

3.6. Enrichment analysis

Pathway enrichment analysis revealed that the identified VMPs/VMRs associated with AD neuropathology were overrepresented in biological processes related to neuron differentiation, neuron projection development, calcium ion transmembrane transport, positive regulation of nervous system development, synaptic membrane, and neuronal postsynaptic density. Moreover, the putative VMR genes were enriched in GWAS loci that were previously implicated in AD (Beecham et al., 2014; Campion et al., 2016; Jun et al., 2016; Sherva et al., 2014). Table 4 shows the top enriched pathways. A full list of the enriched pathways is shown in Table S7. GWAS loci enrichment is shown in Table S8.

3.7. Co-methylation networks

Our network analysis identified 4 co-methylated modules for VMPs/VMRs associated with amyloid-β (Fig. S1A) and 4 modules for those associated with tangles (Fig. S1B). The network structure of 2 modules associated with amyloid-β (brown and yellow) was not preserved, suggesting potential differential networks between

Table 3
Top 50 most significant variably methylated probes (VMPs) associated with tangles (q < 0.05)

CpG probe	Chr	Position (bps)	Genomic features	*p*-value	*q*-value	Gene[a]	Direction[b]
cg21406811	1	51,271,043	Introns	4.08×10^{-12}	1.63×10^{-6}	*FAF1*	↑
cg23067228	15	70,881,206	Intergenic	7.37×10^{-12}	1.63×10^{-6}		↑
cg22895202	14	21,238,166	Promoters	3.11×10^{-11}	4.58×10^{-6}	*EDDM3B*	↑
cg09183598	19	57,679,015	Promoters	5.26×10^{-11}	5.81×10^{-6}	*DUXA*	↑
cg12308275	15	43,558,855	Promoters	1.54×10^{-10}	1.37×10^{-5}	*TGM5*	↑
cg16008918	4	78,740,080	Intergenic	2.03×10^{-10}	1.49×10^{-5}		↑
cg13689497	19	3,201,528	Intergenic	2.82×10^{-9}	1.78×10^{-4}		↑
cg17678740	7	53,254,947	Intergenic	4.36×10^{-9}	2.41×10^{-4}		↓
cg23524184	17	48,129,754	Intergenic	2.75×10^{-8}	1.25×10^{-3}	*ITGA3*	↑
cg22661129	8	35,580,715	Promoters	3.11×10^{-8}	1.25×10^{-3}	*UNC5D*	↑
cg25868285	7	134,455,275	Intergenic	3.12×10^{-8}	1.25×10^{-3}		↑
cg04559604	8	22,031,763	Intergenic	5.34×10^{-8}	1.97×10^{-3}		↑
cg01363574	3	40,354,920	Intergenic	1.03×10^{-7}	3.31×10^{-3}	*EIF1B-AS1*	↑
cg16353628	2	85,239,916	Introns	1.05×10^{-7}	3.31×10^{-3}	*KCMF1*	↑
cg09352908	3	37,017,749	Intergenic	1.23×10^{-7}	3.63×10^{-3}		↓
cg14115740	9	98,054,883	Intergenic	2.16×10^{-7}	5.97×10^{-3}		↓
cg04212651	6	112,671,523	Promoters	2.30×10^{-7}	5.98×10^{-3}	*RFPL4B*	↑
cg02745683	4	3,513,990	Exons	2.60×10^{-7}	6.28×10^{-3}	*LRPAP1*	↑
cg20376421	12	56,546,193	Promoters	2.70×10^{-7}	6.28×10^{-3}	*MYL6B*	↓
cg26227935	18	77,682,412	Intergenic	3.13×10^{-7}	6.91×10^{-3}		↑
cg19729949	5	142,514,108	Intergenic	4.11×10^{-7}	8.66×10^{-3}		↑
cg01869224	12	53,356,063	Intergenic	4.79×10^{-7}	9.13×10^{-3}		↑
cg05929056	21	43,274,690	Intergenic	4.81×10^{-7}	9.13×10^{-3}		↑
cg12538597	11	85,906,334	Intergenic	5.13×10^{-7}	9.13×10^{-3}		↓
cg20660860	2	122,095,855	Exons	5.27×10^{-7}	9.13×10^{-3}	*CLASP1*	↑
cg24663683	5	39,721,720	Intergenic	5.56×10^{-7}	9.13×10^{-3}		↓
cg09537031	8	19,171,706	Intergenic	5.87×10^{-7}	9.13×10^{-3}		↑
cg09828625	20	23,331,259	Promoters	5.97×10^{-7}	9.13×10^{-3}	*NXT1*	↑
cg08866589	5	141,303,260	Promoters	6.02×10^{-7}	9.13×10^{-3}	*KIAA0141*	↑
cg20208633	4	55,405,888	Intergenic	6.19×10^{-7}	9.13×10^{-3}		↑
cg07252851	5	74,063,056	Promoters	6.55×10^{-7}	9.29×10^{-3}	*GFM2*	↓
cg10690677	1	87,019,175	Introns	6.73×10^{-7}	9.29×10^{-3}	*CLCA4*	↓
cg12550816	19	47,163,979	Promoters	7.07×10^{-7}	9.46×10^{-3}	*DACT3-AS1*	↓
cg06159435	11	118,966,351	Promoters	7.31×10^{-7}	9.46×10^{-3}	*H2AFX*	↓
cg13838599	9	128,989,097	Intergenic	7.49×10^{-7}	9.46×10^{-3}		↑
cg06459913	16	11,361,823	Introns	7.93×10^{-7}	9.59×10^{-3}	*RMI2*	↑
cg18803079	1	64,014,643	Promoters	8.03×10^{-7}	9.59×10^{-3}	*EFCAB7*	↓
cg14559409	10	65,930,703	Intergenic	8.87×10^{-7}	1.03×10^{-2}		↓
cg21962918	5	134,094,454	Intergenic	1.00×10^{-6}	1.11×10^{-2}		↓
cg02738677	3	133,265,129	Intergenic	1.01×10^{-6}	1.11×10^{-2}		↓
cg10269358	19	17,728,585	Exons	1.03×10^{-6}	1.11×10^{-2}	*UNC13 A*	↑
cg22331096	8	128,749,328	Introns	1.16×10^{-6}	1.21×10^{-2}	*MYC*	↓
cg01778384	13	27,236,961	Introns	1.20×10^{-6}	1.21×10^{-2}	*WASF3*	↑
cg02746684	3	197,347,276	Introns	1.23×10^{-6}	1.21×10^{-2}	*LOC220729*	↑
cg08450091	3	82,857,215	Intergenic	1.24×10^{-6}	1.21×10^{-2}		↓
cg04005938	7	148,334,417	Intergenic	1.27×10^{-6}	1.21×10^{-2}		↓
cg27618483	2	155,433,424	Intergenic	1.31×10^{-6}	1.21×10^{-2}		↓
cg17095167	13	21,833,918	Intergenic	1.31×10^{-6}	1.21×10^{-2}		↓
cg01757206	17	7,183,913	Intergenic	1.46×10^{-6}	1.32×10^{-2}	*SLC2A4*	↓
cg26342398	1	85,156,326	Promoters	1.61×10^{-6}	1.42×10^{-2}	*SSX2IP*	↓

[a] The nearest annotated gene within ±5 kb of the CpG probe.
[b] ↑ indicates hypervariable (increased variability in subjects with higher neuropathological burden as compared to those with lower burden), and ↓ indicates hypovariable (decreased variability in subjects with higher neuropathological burden as compared to those with lower burden).

patients with high (upper tertile) versus low (bottom tertile) burden for AD pathology (Fig. S2).

3.8. Overlapping between VMPs and DMPs

To compare whether and to what extent the identified VMPs overlap with DMPs, we conducted differential methylation analyses and identified 415 and 3859 DMPs associated with amyloid-β and tangles, respectively (Table S9). Of these, 17.7% of the amyloid-β-related VMPs were also DMPs, whereas 26.1% of the tangle-related VMPs overlapped with DMPs. These results demonstrated that most of the AD-related VMPs were not overlapped with DMPs, implying that VMPs and DMPs may capture different sets of genes and thus may reflect different aspects of AD pathology. In addition, to test whether the overlapping between VMPs and DMPs could be more or less than would expect by chance, we conducted the Fisher's exact test. We obtained highly significant *p*-values for both neuropathological phenotypes (2.17×10^{-80} for amyloid-β, 7.52×10^{-32} for tangles), suggesting that the observed overlapping between VMPs and DMPs should most likely represent true biology rather than chance alone.

3.9. External replication of tangle-related VMPs

Of the 115 tangle-related VMPs identified in ROSMAP, 31 probes were nominally associated with Braak score at a raw *p*-value < 0.05 after adjusting for age at death and gender. Of these, 29 probes (94%) had the same direction (hypervariably/hypovariably methylated) as that in the ROSMAP. However, only 4 probes passed multiple testing at FDR < 0.05. The lack of replication could be due to multiple reasons. First, the sample size used in the external validation was rather small compared to that used in ROSMAP.

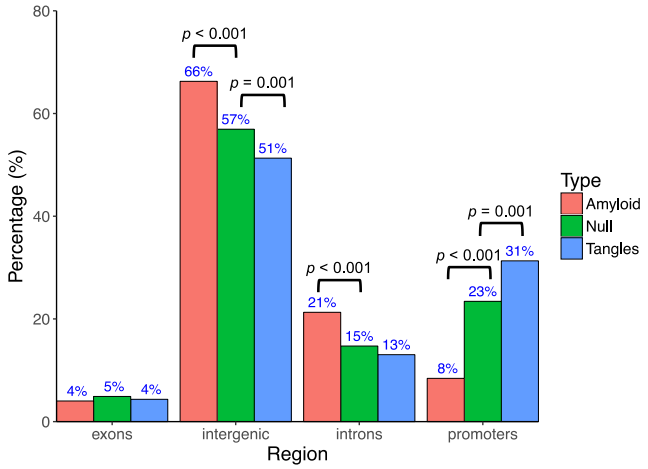

Fig. 2. Genomic distribution of the identified VMPs associated with amyloid-β and tangles. The "null" represents all probes included in the Illumina HumanMethylation450 array. Abbreviation: VMPs, variably methylated probes.

Second, the Braak score included in the publicly available data set is different from the quantitative measure of tangles (quantified by molecularly specific immunohistochemistry across 8 brain regions) used in our analysis. Third, the publicly available data set did not contain information for confounding variables such as education. We were unable to replicate the association of amyloid-related VMPs due to lack of the amyloid phenotype in the external data set.

4. Discussion

In 2 community-based population cohort studies of aging and dementia, we found that the variability in DNA methylation was related to AD neuropathology. Specifically, we identified 249 VMPs (clustered into 133 VMRs) and 115 VMPs (clustered into 14 VMRs) significantly associated with amyloid-β and tangles, respectively. The identified VMR genes were enriched in biological processes related to excitatory synapse, neuron differentiation, calcium ion transmembrane transport, positive regulation of nervous system development, and neuronal postsynaptic density. Our results support a role of DNA methylation variability in AD pathology and highlight the importance of testing DNA methylation variability in epigenetic research.

Of the identified VMR genes, the *TUBGCP3* gene showed the strongest association with amyloid-β. This gene encodes the tubulin gamma complex associated protein 3 and is expressed in multiple brain regions. It plays an important role in microtubule nucleation, reduction of which may contribute to neuronal degeneration (Cash et al., 2003; Jean and Baas, 2013). Another VMR gene is *NGFR*, which acts as a proapoptotic receptor in neuron cell death via binding to Aβ in the AD brain (Lee et al., 2001). Genetic polymorphisms of this gene were associated with AD (Cozza et al., 2008). Other top-ranked VMR genes include *CCR3* (Leung et al., 2013; Villeda et al., 2011; Zhu et al., 2017), *C10orf54* (De Jager et al., 2014; Lord and Cruchaga, 2014), and *WDR81* (De Jager et al., 2014; Kauwe et al., 2014), many of which have been previously associated with cognitive impairment and/or AD pathology. The most significant VMR gene associated with tangles was *FAF1*, which is a *fas*-binding protein that plays an important role in neurodevelopment (Menges et al., 2009), neurodegeneration (Sul et al., 2013), and tumorigenesis (Menges et al., 2009). The second gene showing strong variable methylation in relation to tangles was *LRPAP1*. This gene encodes a protein that interacts with low density lipoprotein receptor–related protein (LRP) that plays a critical role in brain Aβ clearance (Kanekiyo et al., 2013). Moreover, genetic polymorphisms in *LRPAP1* were associated with AD (Sánchez et al., 2001). Another

Table 4
Top 30 enriched pathways related to Alzheimer's disease neuropathology

Pathway/GO terms	q-value[a]	
	Amyloid-β	Tangles
Regulation of neuron projection development	3.88×10^{-12}	3.43×10^{-12}
Calcium ion transmembrane transporter activity	2.10×10^{-9}	2.42×10^{-5}
Postsynapse	6.94×10^{-9}	8.00×10^{-11}
Calcium ion transmembrane transport	1.04×10^{-8}	1.16×10^{-4}
Positive regulation of cell projection organization	1.73×10^{-8}	4.03×10^{-7}
Positive regulation of neuron projection development	2.48×10^{-8}	4.07×10^{-8}
Cell leading edge	2.94×10^{-8}	4.22×10^{-8}
Positive regulation of neuron differentiation	8.55×10^{-8}	6.84×10^{-8}
Divalent inorganic cation transmembrane transporter activity	2.71×10^{-7}	1.69×10^{-3}
Calcium ion transport	1.29×10^{-6}	8.72×10^{-5}
Actin binding	1.51×10^{-6}	4.07×10^{-8}
Reactome: axon guidance	2.15×10^{-6}	1.19×10^{-5}
Positive regulation of nervous system development	3.77×10^{-6}	4.36×10^{-7}
Cell projection membrane	5.90×10^{-6}	2.04×10^{-6}
Divalent inorganic cation transport	5.90×10^{-6}	6.08×10^{-4}
Regulation of dendrite development	8.98×10^{-6}	1.60×10^{-4}
Gtpase binding	9.91×10^{-6}	6.31×10^{-5}
Synaptic membrane	1.02×10^{-5}	4.07×10^{-8}
Guanyl nucleotide exchange factor activity	1.21×10^{-5}	6.84×10^{-8}
Main axon	1.55×10^{-5}	8.56×10^{-4}
Excitatory synapse	2.39×10^{-5}	2.93×10^{-9}
Regulation of small gtpase mediated signal transduction	2.39×10^{-5}	1.08×10^{-6}
Regulation of cell morphogenesis involved in differentiation	8.82×10^{-5}	4.36×10^{-7}
Cation channel activity	1.17×10^{-4}	1.31×10^{-6}
Neuron projection morphogenesis	1.31×10^{-4}	4.03×10^{-7}
Axon	1.33×10^{-4}	9.97×10^{-8}
Receptor complex	2.27×10^{-4}	1.50×10^{-6}
Ras guanyl nucleotide exchange factor activity	1.42×10^{-3}	4.36×10^{-7}
Gated channel activity	3.47×10^{-3}	1.06×10^{-7}
Neuronal postsynaptic density	3.99×10^{-2}	1.11×10^{-6}

[a] Adjusted for multiple testing by the Benjamini-Hochberg method.

VMR gene associated with tangles was *MYC*, a proto-oncogene that encodes a nuclear phosphoprotein that plays a role in cell cycle progression, apoptosis, and cellular transformation (Dang, 1999). In a mouse model, neuronal expression of *MYC* causes a neurodegenerative phenotype (Lee et al., 2009). Moreover, there is evidence demonstrating that *MYC* might be a key regulator of cell cycle–mediated neuronal cell death (Lee et al., 2009). Notably, some of the VMR genes may contribute to AD pathology through changing variability, but not mean level of DNA methylation, and thus would otherwise be missed by testing DMPs only.

Our network analysis identified 2 modules (the brown module and yellow module). The hub genes of these networks highlight the potential role of *HOXA3* and *HOXA5* in AD pathology. This is corroborated by previous evidence demonstrating that expression of the *HOX* family genes plays critical roles in the formation and function of the central nervous system (Lizen et al., 2017; Rezsohazy et al., 2015) and is also in line with a recent study demonstrating that elevated DNA methylation level of the *HOXA* genes was associated with AD neuropathology (Smith et al., 2018). Although the current analysis and previous studies (Hansen et al., 2011; Jones et al., 2015; Paul et al., 2016; Webster et al., 2018) suggest a potential important role of altered DNA methylation variability in human diseases, the biological mechanisms behind the observed associations remain to be determined. It is possible that altered DNA methylation stability may reflect the exposure of disease risk factors, and thus, differential methylation variability could represent the different exposure profiles of these factors between cases and controls (Teschendorff et al., 2012). It is also possible that the altered DNA methylation variability could represent beneficial adaptions in response of disease process (Feinberg and Irizarry, 2010; Hansen et al., 2011). Further research is needed to test these hypotheses.

Several aspects of our findings deserve discussions. First, although we found that some genes showed differential methylation at both the mean and variance levels, for example, about 18% and 26% of the VMPs associated with amyloid-β and tangles, respectively, overlapped with the DMPs. However, many genes showed either variable methylation or differential mean methylation, but not both. For instance, most of the identified VMPs (more than 70%) did not overlap with those DMPs detected based on mean DNA methylation analysis. These observations indicate that VMPs and DMPs analyses capture different sets of genes associated with AD pathology, and thus, both mean and variance should be tested in epigenetic analysis. Statistical analysis that tests only the mean DNA methylation level without considering variability will miss important disease-related genes. Second, the VMPs/VMRs identified in the present study most likely represented true biological variability instead of technical artifacts because (1) many VMR genes, especially those associated with tangles, also showed differential expression; (2) the identified VMR genes were significantly overrepresented in excitatory synapse, and neuron differentiation, calcium ion transmembrane transport, and so on. Moreover, these VMR genes were enriched in previous GWAS loci for AD (Beecham et al., 2014; Jun et al., 2016; Sherva et al., 2014). Third, as part of the QC procedures, we compared DMPs identified in this study with those reported in previous EWAS in the same brain cortex (De Jager et al., 2014). We found that 65.4% of the DMPs identified in the current analysis overlapped with previously reported probes associated with neuritic plaque (De Jager et al., 2014), demonstrating the credibility of our QC procedures used in the current analysis. However, the DMPs identified in the current analysis are not identical to those reported previously by De Jager et al. (2014) due to the following reasons: (1) different preprocessing pipeline/QC criteria and thus different number and sets of initial probes included in the final data analysis; (2) slightly different phenotypes used in the 2 studies. In the work by De Jager et al. (2014), the authors used neuritic plaque quantified by microscopic examination of silver-stained slides from 5 brain regions (midfrontal cortex, midtemporal cortex, inferior parietal cortex, entorhinal cortex, and hippocampus), whereas in our analysis, we used a composite measure of neuropathological burden quantified by molecularly specific immunohistochemistry across 8 brain regions (hippocampus, entorhinal cortex, midfrontal gyrus, inferior temporal, anterior gyrus, calcarine cortex, cingulate region, and superior frontal gyrus); and (3) different statistical models along with different covariates adjustments. Fourth, our results demonstrate that the 2 AD hallmarks—amyloid-β and tangles—are etiologically highly heterogeneous. For instance, of the identified VMPs associated with either amyloid-β or tangles, only 1 probe (*cg01869224*) associates with both traits. Moreover, we observed differential genomic distribution of the VMPs associated with amyloid-β or tangles, that is, amyloid-β-associated VMPs are largely enriched in introns and intergenic regions but depleted in promoter regions, whereas those associated with neurofibrillary tangles are overrepresented in promoters but depleted in intergenic regions. Although the mechanisms behind the observed trait-specific distribution of these VMPs are unclear, it is possible that DNA methylation variability of probes located in the promoter regions may have a larger impact on gene expression than those located in the introns/intergenic regions (Lee and Wiemels, 2015; Suzuki and Bird, 2008). In line with this hypothesis, majority (62.5%) of the VMR genes associated with tangles are differentially expressed, whereas only a small proportion (1.8%) of the amyloid-β-associated VMR genes showed differential expression. The observed trait-specific genomic distributions of the identified VMPs also suggest that the 2 hallmarks of AD (i.e., amyloid plaque and tangle) may be etiologically heterogeneous. Fifth, nearly 90% of the amyloid-β-associated VMPs are hypervariable probes, whereas majority (~58%) of the tangle-related VMPs are hypovariable ones. Although these observations support a role of DNA methylation variability in gene regulation and AD pathogenesis, our findings unravel the etiological heterogeneity of the 2 hallmarks, and highlight the importance of studying both traits in future research. Finally, because the relationship between gene expression and DNA methylation is not one-on-one, it is possible that DNA methylation variability affects the 2 phenotypes through different biological pathways. Together, our findings suggest that the relationship between DNA methylation variability and gene expression in the human AD brain may be trait specific.

Our study has several limitations. First, the present study only examined VMRs in 1 brain region (prefrontal cortex), but it is possible that DNA methylation variability varies across different brain regions. Future research should investigate the region-specific effect of DNA methylation variability on AD pathology. Second, participants included in the current analysis are highly educated European Caucasians, and our results may not be generalized to other ethnic groups or population settings. Third, the identified association between DNA methylation variability and AD pathology do not imply causality.

However, our study has several strengths. To our knowledge, this is the first study examining the association between variably methylated probes/regions and AD neuropathology in a large collection of postmortem human brains. Moreover, we conducted statistical analyses including differentially variably methylation analysis, functional annotation analysis, pathway enrichment analysis, and co-methylation network analysis. Furthermore, we studied different neuropathological phenotypes, for example, amyloid-β and tangles, and identified trait-specific association of variably methylated genes with AD neuropathology.

Disclosure

The authors have no conflicts of interest to declare.

Acknowledgements

The authors would like to thank the participants of the Religious Orders Study and Memory and Aging Project studies and the staff of the Rush Alzheimer's Disease Center.

This work was supported by the National Institutes of Health grants RF1AG52476, P30AG10161, RF1AG15819, R01AG17917, R01AG16042, U01AG46152, RF1AG36042, and R01AG36836.

Appendix A. Supplementary data

Supplementary data associated with this article can be found, in the online version, at https://doi.org/10.1016/j.neurobiolaging.2018.12.003.

References

Aryee, M.J., Jaffe, A.E., Corrada-Bravo, H., Ladd-Acosta, C., Feinberg, A.P., Hansen, K.D., Irizarry, R.A., 2014. Minfi: a flexible and comprehensive Bioconductor package for the analysis of infinium DNA methylation microarrays. Bioinformatics 30, 1363–1369.

Assenov, Y., Müller, F., Lutsik, P., Walter, J., Lengauer, T., Bock, C., 2014. Comprehensive analysis of DNA methylation data with RnBeads. Nat. Methods 11, 1138.

Beecham, G.W., Hamilton, K., Naj, A.C., Martin, E.R., Huentelman, M., Myers, A.J., Corneveaux, J.J., Hardy, J., Vonsattel, J.-P., Younkin, S.G., others, 2014. Genome-wide association meta-analysis of neuropathologic features of Alzheimer's disease and related dementias. PLoS Genet. 10, e1004606.

Benjamini, Y., Hochberg, Y., 1995. Controlling the false discovery rate: a practical and powerful approach to multiple testing. J. Royal Stat. Soc. Ser. B 289–300.

Bennett, D.A., Schneider, J.A., Wilson, R.S., Bienias, J.L., Arnold, S.E., 2004. Neurofibrillary tangles mediate the association of amyloid load with clinical Alzheimer disease and level of cognitive function. Arch. Neurol. 61, 378–384.

Bennett, D.A., Schneider, J.A., Arvanitakis, Z., Kelly, J.F., Aggarwal, N.T., Shah, R.C., Wilson, R.S., 2006. Neuropathology of older persons without cognitive impairment from two community-based studies. Neurology 66, 1837–1844.

Bennett, D.A., De Jager, P.L., Leurgans, S.E., Schneider, J.A., 2009. Neuropathologic intermediate phenotypes enhance association to Alzheimer susceptibility alleles. Neurology 72, 1495–1503.

Bennett, D.A., Schneider, J.A., Arvanitakis, Z., Wilson, R.S., 2012a. Overview and findings from the religious orders study. Curr. Alzheimer Res. 9, 628–645.

Bennett, D.A., Schneider, J.A., Buchman, A., Barnes, L., Boyle, P.A., Wilson, R.S., 2012b. Overview and findings from the rush memory and aging project. Curr. Alzheimer Res. 9, 646–663.

Brown, M.B., 1975. 400: a method for combining non-independent, one-sided tests of significance. Biometrics 987–992.

Campion, D., Pottier, C., Nicolas, G., Le Guennec, K., Rovelet-Lecrux, A., 2016. Alzheimer disease: modeling an A$β$-centered biological network. Mol. Psychiatry 21, 861.

Cash, A.D., Aliev, G., Siedlak, S.L., Nunomura, A., Fujioka, H., Zhu, X., Raina, A.K., Vinters, H.V., Tabaton, M., Johnson, A.B., others, 2003. Microtubule reduction in Alzheimer's disease and aging is independent of $τ$ filament formation. Am. J. Pathol. 162, 1623–1627.

Cozza, A., Melissari, E., Iacopetti, P., Mariotti, V., Tedde, A., Nacmias, B., Conte, A., Sorbi, S., Pellegrini, S., 2008. SNPs in neurotrophin system genes and Alzheimer's disease in an Italian population. J. Alzheimers Dis. 15, 61–70.

Csardi, G., Nepusz, T., 2006. The igraph software package for complex network research. InterJournal Complex Syst. 1695, 1–9.

Dang, C.V., 1999. c-Myc target genes involved in cell growth, apoptosis, and metabolism. Mol. Cell. Biol. 19, 1–11.

De Jager, P.L., Srivastava, G., Lunnon, K., Burgess, J., Schalkwyk, L.C., Yu, L., Eaton, M.L., Keenan, B.T., Ernst, J., McCabe, C., others, 2014. Alzheimer's disease: early alterations in brain DNA methylation at ANK1, BIN1, RHBDF2 and other loci. Nat. Neurosci. 17, 1156.

Duthey, B., 2013. Background paper 6.11: Alzheimer disease and other dementias. In: A Public Health Approach to Innovation. World Health Organization, Geneva, Switzerland, pp. 1–74.

Feinberg, A.P., Irizarry, R.A., 2010. Stochastic epigenetic variation as a driving force of development, evolutionary adaptation, and disease. Proc. Natl. Acad. Sci. U S A 107, 1757–1764.

Guintivano, J., Aryee, M.J., Kaminsky, Z.A., 2013. A cell epigenotype specific model for the correction of brain cellular heterogeneity bias and its application to age, brain region and major depression. Epigenetics 8, 290–302.

Hansen, K.D., Timp, W., Bravo, H.C., Sabunciyan, S., Langmead, B., McDonald, O.G., Wen, B., Wu, H., Liu, Y., Diep, D., others, 2011. Increased methylation variation in epigenetic domains across cancer types. Nat. Genet. 43, 768.

Hastie, T., Tibshirani, R., Narasimhan, B., Chu, G., 2001. impute: imputation for microarray data. Bioinformatics 17, 520–525.

Irier, H.A., Jin, P., 2012. Dynamics of DNA methylation in aging and Alzheimer's disease. DNA Cell Biol. 31, S42–S48.

Jean, D.C., Baas, P.W., 2013. It cuts two ways: microtubule loss during Alzheimer disease. EMBO J. 32, 2900–2902.

Jones, M.J., Goodman, S.J., Kobor, M.S., 2015. DNA methylation and healthy human aging. Aging Cell 14, 924–932.

Jun, G., Ibrahim-Verbaas, C.A., Vronskaya, M., Lambert, J.-C., Chung, J., Naj, A.C., Kunkle, B.W., Wang, L.-S., Bis, J.C., Bellenguez, C., others, 2016. A novel Alzheimer disease locus located near the gene encoding tau protein. Mol. Psychiatry 21, 108.

Kanekiyo, T., Cirrito, J.R., Liu, C.-C., Shinohara, M., Li, J., Schuler, D.R., Shinohara, M., Holtzman, D.M., Bu, G., 2013. Neuronal clearance of amyloid-$β$ by endocytic receptor LRP1. J. Neurosci. 33, 19276–19283.

Kauwe, J.S.K., Bailey, M.H., Ridge, P.G., Perry, R., Wadsworth, M.E., Hoyt, K.L., Staley, L.A., Karch, C.M., Harari, O., Cruchaga, C., others, 2014. Genome-wide association study of CSF levels of 59 Alzheimer's disease candidate proteins: significant associations with proteins involved in amyloid processing and inflammation. PLoS Genet. 10, e1004758.

Langfelder, P., Horvath, S., 2008. WGCNA: an R package for weighted correlation network analysis. BMC Bioinformatics 9, 559.

Lawrence, M., Huber, W., Pages, H., Aboyoun, P., Carlson, M., Gentleman, R., Morgan, M.T., Carey, V.J., 2013. Software for computing and annotating genomic ranges. PLoS Comput. Biol. 9, e1003118.

Lee, R., Kermani, P., Teng, K.K., Hempstead, B.L., 2001. Regulation of cell survival by secreted proneurotrophins. Science 294, 1945–1948.

Lee, H., Casadesus, G., Nunomura, A., Zhu, X., Castellani, R.J., Richardson, S.L., Perry, G., Felsher, D.W., Petersen, R.B., Smith, M.A., 2009. The neuronal expression of MYC causes a neurodegenerative phenotype in a novel transgenic mouse. Am. J. Pathol. 174, 891–897.

Lee, S.-T., Wiemels, J.L., 2015. Genome-wide CpG island methylation and intergenic demethylation propensities vary among different tumor sites. Nucleic Acids Res. 44, 1105–1117.

Leung, R., Proitsi, P., Simmons, A., Lunnon, K., Güntert, A., Kronenberg, D., Pritchard, M., Tsolaki, M., Mecocci, P., Kloszewska, I., others, 2013. Inflammatory proteins in plasma are associated with severity of Alzheimer's disease. PLoS One 8, e64971.

Lizen, B., Moens, C., Mouheiche, J., Sacré, T., Ahn, M.-T., Jeannotte, L., Salti, A., Gofflot, F., 2017. Conditional loss of Hoxa5 function early after birth impacts on expression of genes with synaptic function. Front. Mol. Neurosci. 10, 369.

Lord, J., Cruchaga, C., 2014. The epigenetic landscape of Alzheimer's disease. Nat. Neurosci. 17, 1138.

Lunnon, K., Smith, R., Hannon, E., De Jager, P.L., Srivastava, G., Volta, M., Troakes, C., Al-Sarraj, S., Burrage, J., Macdonald, R., others, 2014. Methylomic profiling implicates cortical deregulation of ANK1 in Alzheimer's disease. Nat. Neurosci. 17, 1164.

Margolin, A.A., Nemenman, I., Basso, K., Wiggins, C., Stolovitzky, G., Dalla Favera, R., Califano, A., 2006. ARACNE: an algorithm for the reconstruction of gene regulatory networks in a mammalian cellular context. BMC Bioinformatics S7.

Menges, C.W., Altomare, D.A., Testa, J.R., 2009. FAS-associated factor 1 (FAF1): diverse functions and implications for oncogenesis. Cell Cycle 8, 2528–2534.

Meyer, P.E., Lafitte, F., Bontempi, G., 2008. Minet: an open source R/Bioconductor package for mutual information based network inference. BMC Bioinformatics 9, 461.

Palumbo, D., Affinito, O., Monticelli, A., Cocozza, S., 2018. DNA Methylation variability among individuals is related to CpGs cluster density and evolutionary signatures. BMC Genomics 19, 229.

Paul, D.S., Teschendorff, A.E., Dang, M.A.N., Lowe, R., Hawa, M.I., Ecker, S., Beyan, H., Cunningham, S., Fouts, A.R., Ramelius, A., others, 2016. Increased DNA methylation variability in type 1 diabetes across three immune effector cell types. Nat. Commun. 7, 13555.

Phipson, B., Maksimovic, J., Oshlack, A., 2015. missMethyl: an R package for analyzing data from Illumina's HumanMethylation450 platform. Bioinformatics 32, 286–288.

Phipson, B., Oshlack, A., 2014. DiffVar: a new method for detecting differential variability with application to methylation in cancer and aging. Genome Biol. 15, 465.

Poole, W., Gibbs, D.L., Shmulevich, I., Bernard, B., Knijnenburg, T.A., 2016. Combining dependent P-values with an empirical adaptation of Brown's method. Bioinformatics 32, i430–i436.

Rezsohazy, R., Saurin, A.J., Maurel-Zaffran, C., Graba, Y., 2015. Cellular and molecular insights into Hox protein action. Development 142, 1212–1227.

Saffari, A., Silver, M.J., Zavattari, P., Moi, L., Columbano, A., Meaburn, E.L., Dudbridge, F., 2018. Estimation of a significance threshold for epigenome-wide association studies. Genet. Epidemiol. 42, 20–33.

Sánchez, L., Alvarez, V., González, P., González, I., Alvarez, R., Coto, E., 2001. Variation in the LRP-associated protein gene (LRPAP1) is associated with late-onset Alzheimer disease. Am. J. Med. Genet. 105, 76–78.

Sherva, R., Tripodis, Y., Bennett, D.A., Chibnik, L.B., Crane, P.K., De Jager, P.L., Farrer, L.A., Saykin, A.J., Shulman, J.M., Naj, A., others, 2014. Genome-wide association study of the rate of cognitive decline in Alzheimer's disease. Alzheimers Dement. 10, 45–52.

Smith, R.G., Hannon, E., De Jager, P.L., Chibnik, L., Lott, S.J., Condliffe, D., Smith, A.R., Haroutunian, V., Troakes, C., Al-Sarraj, S., others, 2018. Elevated DNA methylation across a 48-kb region spanning the HOXA gene cluster is associated with Alzheimer's disease neuropathology. Alzheimers Dement 14, 1580–1588.

Smyth, G.K., 2005. Limma: Linear Models for Microarray Data, in: Bioinformatics and Computational Biology Solutions Using R and Bioconductor. Springer, New York, NY, pp. 397–420.

Stephens, M.A., 1974. EDF statistics for goodness of fit and some comparisons. J. Am. Stat. Assoc. 69, 730–737.

Sul, J.-W., Park, M.-Y., Shin, J., Kim, Y.-R., Yoo, S.-E., Kong, Y.-Y., Kwon, K.-S., Lee, Y.H., Kim, E., 2013. Accumulation of the parkin substrate, FAF1, plays a key role in the dopaminergic neurodegeneration. Hum. Mol. Genet. 22, 1558–1573.

Suzuki, M.M., Bird, A., 2008. DNA methylation landscapes: provocative insights from epigenomics. Nat. Rev. Genet. 9, 465.

Teschendorff, A.E., Jones, A., Fiegl, H., Sargent, A., Zhuang, J.J., Kitchener, H.C., Widschwendter, M., 2012. Epigenetic variability in cells of normal cytology is associated with the risk of future morphological transformation. Genome Med. 4, 24.

Villeda, S.A., Luo, J., Mosher, K.I., Zou, B., Britschgi, M., Bieri, G., Stan, T.M., Fainberg, N., Ding, Z., Eggel, A., others, 2011. The ageing systemic milieu negatively regulates neurogenesis and cognitive function. Nature 477, 90.

Watson, C.T., Roussos, P., Garg, P., Ho, D.J., Azam, N., Katsel, P.L., Haroutunian, V., Sharp, A.J., 2016. Genome-wide DNA methylation profiling in the superior temporal gyrus reveals epigenetic signatures associated with Alzheimer's disease. Genome Med. 8, 5.

Webster, A.P., Plant, D., Ecker, S., Zufferey, F., Bell, J.T., Feber, A., Paul, D.S., Beck, S., Barton, A., Williams, F.M.K., others, 2018. Increased DNA Methylation Variability in Rheumatoid Arthritis Discordant Monozygotic Twins bioRxiv 314963.

Welter, D., MacArthur, J., Morales, J., Burdett, T., Hall, P., Junkins, H., Klemm, A., Flicek, P., Manolio, T., Hindorff, L., others, 2013. The NHGRI GWAS Catalog, a curated resource of SNP-trait associations. Nucleic Acids Res. 42, D1001–D1006.

Wilson, R.S., Boyle, P.A., Yu, L., Barnes, L.L., Sytsma, J., Buchman, A.S., Bennett, D.A., Schneider, J.A., 2015. Temporal course and pathologic basis of unawareness of memory loss in dementia. Neurology 85, 984–991.

Yang, J., Weedon, M.N., Purcell, S., Lettre, G., Estrada, K., Willer, C.J., Smith, A.V., Ingelsson, E., O'connell, J.R., Mangino, M., others, 2011. Genomic inflation factors under polygenic inheritance. Eur. J. Hum. Genet. 19, 807.

Zhu, C., Xu, B., Sun, X., Zhu, Q., Sui, Y., 2017. Targeting CCR3 to reduce Amyloid-$β$ production, tau hyperphosphorylation, and synaptic loss in a mouse model of Alzheimer's disease. Mol. Neurobiol. 54, 7964–7978.